Structural Eng./Earthquake Eng., JSCE, Vol. 17, No. 2, 163s-174s, 2000 July
(J. Struct. Mech. Earthquake Eng., JSCE, No. 654/ I-52)

PERFORMANCE OF THE QUAY WALL WITH HIGH SEISMIC RESISTANCE

Koji ICHII[1], Susumu IAI[2] and Toshikazu MORITA[3]

[1]Member of JSCE, M.Eng., Research Engineer, Port and Harbour Research Institute, Ministry of Transport
(Nagase 3-1-1, Yokosuka 239-0831, Japan)
[2] Member of JSCE, Dr.Eng., Chief of Disaster Prevention Laboratory, Port and Harbour Research Institute
[3] Member of JSCE, Research Engineer, Port and Harbour Research Institute Ministry of Transport

A high seismic resistance quay wall experienced the 1995 Hyogo-ken nambu earthquake and survived the disaster. To clarify whether high seismic resistance quay walls can survive future earthquakes, a series of two-dimensional effective stress analyses is conducted. The numerical analyses reveal the mechanism why the high seismic resistance quay wall in Kobe Port survived. The numerical results also indicate that it is possible to significantly reduce the residual deformation of quay wall designed with high seismic coefficient if soil improvement against liquefaction is completed.

Key Words : *quay wall, liquefaction, deformation, seismic coefficient*

1. INTRODUCTION

On January 17, 1995, one of the most disastrous earthquakes called the 1995 Hyogoken-nambu earthquake of JMA Magnitude 7.2, hit the Hanshin area of Japan. Kobe Port was shaken with a strong motion having peak ground acceleration of 0.54g and 0.45g in the horizontal and vertical directions respectively[1]. Most of the quay walls in Kobe Port are of a rigid block type made of concrete caissons and were severely damaged by the earthquake. Quay walls moved about 5 m maximum, about 3 m on average, toward the sea. The walls also settled about 1 to 2 m and tilted about 4 degrees toward the sea. The mechanism of this large deformation was identified using effective stress analyses[2] and shaking table tests [3].

One quay wall at Maya Wharf was designed with a high seismic coefficient (K_h=0.25) and available for emergency use just after the earthquake disaster. Although the usual type quay walls were severely damaged, this high seismic resistance quay wall survived and was available for emergency use. This success of a high seismic resistance quay wall encouraged the construction of seismic resistance type quay walls in Japanese ports.

The mechanism of survival of the quay wall designed with high seismic resistance has not been identified. It is necessary to identify why this high seismic resistance quay wall survived and whether or not the same type of quay wall can survive in other earthquakes. In this paper, two-dimensional effective stress analyses are conducted to identify the deformation mechanism and determine why the high seismic resistance quay wall did not suffer severe deformation and damage.

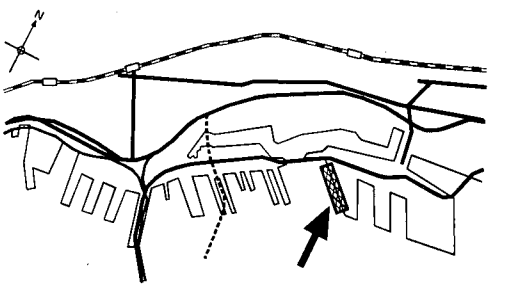

Fig.1 Location of high seismic resistance quay walls at Maya Wharf in Kobe Port.

2. HIGH SEISMIC RESISTANCE QUAY WALL IN KOBE PORT

The location of the high seismic resistance quay wall at Maya Wharf is shown in **Figure 1**. It is located in the northern part of Kobe Port and the quay walls were constructed as steel cellular type quay walls in 1967. After construction of the original

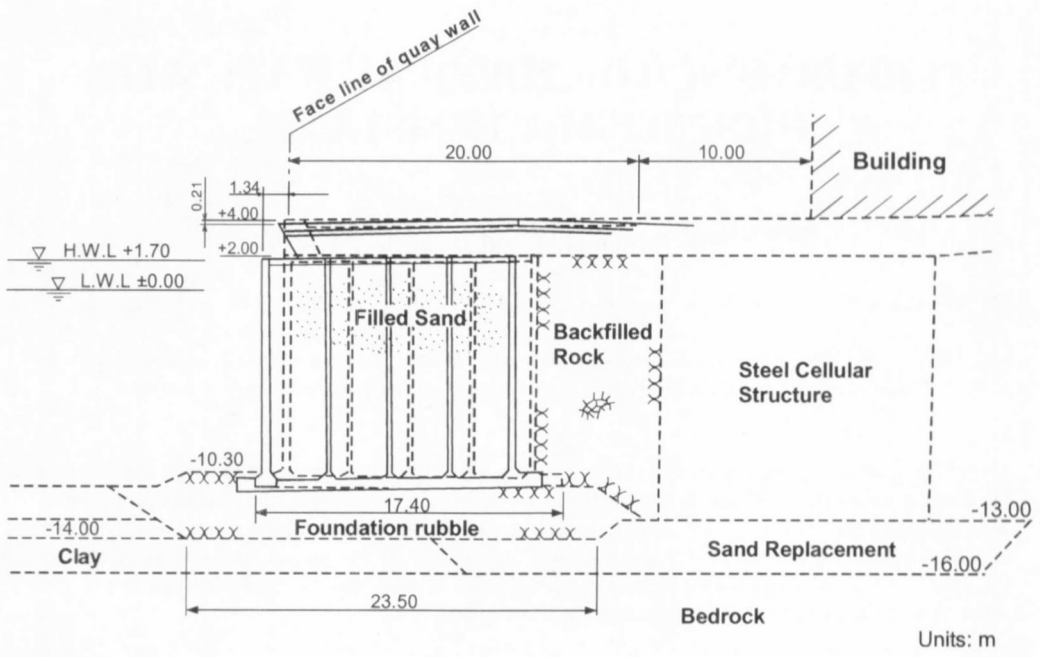

Fig.2 Cross section and deformation of high seismic resistance quay wall.

cellular type quay wall, three berths in Maya No.1 Wharf were improved as high seismic resistance quay walls with seismic coefficients of K_h=0.25. The northern berth of –10 m depth was improved as a pier type quay wall and the other two berths of –10 m depth and –12 m depth were improved as caisson type quay walls. The cross section of the high seismic resistance design quay wall of –10 m depth is shown in **Figure 2**. The old cellular structure still remains behind the caisson and backfill rock was placed between the caisson and the steel cellular structure. The foundation of the old cellular structure was improved with filled sand and the foundation of the caisson was improved with a gravel mound. Though most of the caisson type quay walls in Kobe Port are constructed on the deep clay layer improved with soil replacement, quay walls in Maya Wharf have a shallow clay layer to be improved.

The deformation of the quay walls after the earthquake shaking is also shown in **Figure 2**. The concrete caisson is slightly inclined and moved about 1 to 2 m toward sea. Though horizontal displacement of 1 to 2 m toward the sea and settlement of tens of centimeters occurred, irregularity of displacement was not significant and the quay walls could be used immediately following the earthquake, as shown in **Photo 1**. Since the deformation of the quay walls was very limited and no irregular deformation was observed, it can be concluded that the quay walls didn't suffer significant damage.

Whereas the high seismic resistance quay walls did not suffer significant damage, usual type quay walls in Kobe Port were severely damaged. The displacements of quay walls at Port Island and Rokko Island are shown on **Figure 3**. Quay walls moved 5 m in maximum and about 3 m on average[1]. The mechanism explains the differences in seismic performance has not been identified and

Photo 1 High seismic designed quay walls just after the earthquake.

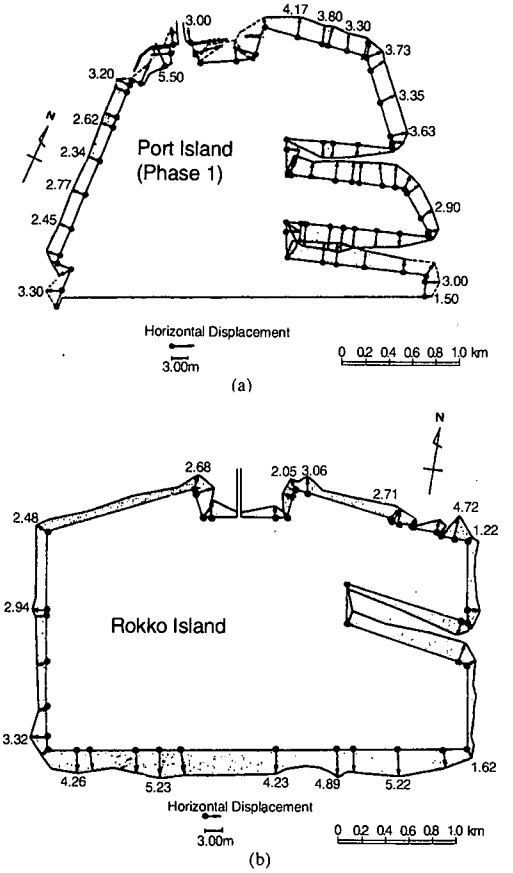

Fig.3 Displacement of quay walls at Port Island and Rokko Island.

there are several factors which affect the seismic performance of the high seismic resistance quay walls. For instance, the horizontal earthquake motion has a predominantly north-south direction as shown in **Figure 4**[4] and the damage of quay walls facing north or south are more severe than that of the quay walls facing east or west direction as shown in **Figure 3**. Since the high seismic resistance quay walls in Maya Wharf have a north-south face line (facing west direction) as shown in **Figure 1**, It is thought that the orientation of the face line parallel to the predominant horizontal direction of earthquake shaking is one of the reasons why these quay walls survived.

The possible factors which may have resulted in a lower deformation of quay walls are summarized as follows.

(1) High seismic coefficient (Kh=0.25)
(2) Existence of old steel cellular structure behind caisson
(3) Absence of weak foundation as liquefiable sand replacement under the caisson
(4) Face line of quay walls parallel to the predominant direction of earthquake shaking.

Therefore, why the high seismic designed quay walls survived in the earthquake is one of the most important issues to be discussed.

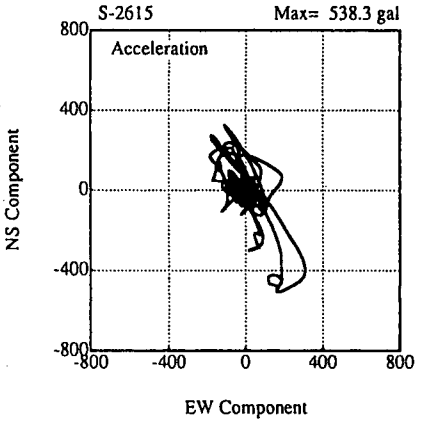

Fig.4 Orbit of acceleration in Kobe Port.

3. OUTLINE OF THE EFFECTIVE STRESS ANALYSIS METHOD

(1) Constitutive Equations

The constitutive model used in this study is a strain space plasticity type and consists of a multiple shear mechanism in the plane strain condition[5]. With the effective stress and strain vectors written by

$$\{\sigma'\}^T = \{\sigma'_x, \sigma'_y, \tau'_{xy}\} \quad (1)$$

$$\{\varepsilon\}^T = \{\varepsilon_x, \varepsilon_y, \gamma_{xy}\} \quad (2)$$

The basic form of the constitutive relation is given by

$$\{d\sigma'\} = [D](\{d\varepsilon\} - \{d\varepsilon_p\}) \quad (3)$$

in which

$$[D] = K\{n^{(0)}\}\{n^{(0)}\}^T + \sum_{i=1}^{I} R_{L/U}^{(i)} \{n^{(i)}\}\{n^{(i)}\}^T \quad (4)$$

In this relation, the term $\{d\varepsilon_p\}$ in Eq.(3) represents the additional strain incremental vector to take the dilatancy into account and is given from the volumetric strain increment due to the dilatancy as

$$\{d\varepsilon_p\}^T = \{d\varepsilon_p / 2, d\varepsilon_p / 2, 0\} \quad (5)$$

The first term in Eq.(4) represents the volumetric mechanism with rebound modulus K and the direction vector is given by

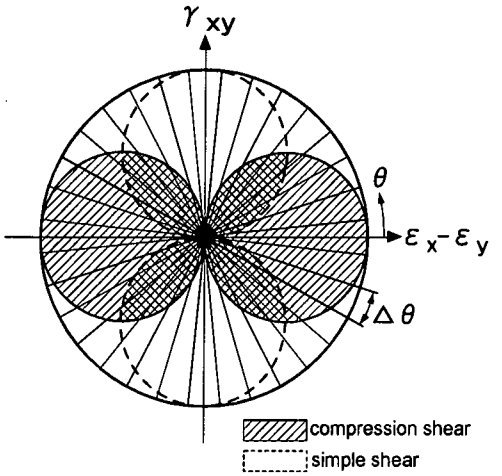

Fig.5 Schematic figure for the multiple simple shear mechanism.

$$\left\{n^{(0)}\right\}^T = \{1,1,0\} \tag{6}$$

The second term in Eq.(4) represents the multiple shear mechanism. Each mechanism i = 1,2,...,I represents a virtual simple shear mechanism, with each simple shear plane oriented at an angle $\theta_i / 2 + \pi / 4$ relative to the x axis.

The tangential shear modulus $R_{L/U}^{(i)}$ represents the hyperbolic stress strain relationship with hysteresis characteristics. The direction vectors for the multiple shear mechanism in Eq.(4) are given by

$$\left\{n^{(i)}\right\}^T = \{\cos\theta_i, -\cos\theta_i, \sin\theta_i\} \tag{7}$$

(for i=1,2,...,I)

in which

$$\theta_i = (i-1)\Delta\theta \qquad \text{(for i=1,2,...,I)} \tag{8}$$

$$\Delta\theta = \pi / I \tag{9}$$

A schematic figure for the multiple simple shear mechanism is shown in **Figure 5**. Pairs of circles indicate mobilized virtual shear strain in positive and negative modes of compression shear (solid lines with darker hatching) and simple shear (broken lines with lighter hatching).

The loading and unloading for the shear mechanism are separately defined for each virtual simple shear mechanism by the sign of $\left\{n^{(i)}\right\}^T \{d\varepsilon\}$. The multiple shear mechanism takes into account the effect of rotation of the principal stress axis directions, the effect of which is known to play an important role in the cyclic behavior of anisotropically consolidated sand[6].

Table 1 Parameters of the present model

Parameters	Type of Mechanism	Kind of the parameters
K_a	Elastic volumetric	Rebound modulus
G_{ma}	Elastic shear	Shear modulus
ϕ_f	Plastic shear	Shear resistance angle
ϕ_p	Plastic dilatancy	Phase transformation angle
H_m	Plastic shear	Hysteretic damting factor at large shear strain level
p_1	Plastic dilatancy	Initial phase of dilatancy
p_2	Plastic dilatancy	Final phase of dilatancy
w_1	Plastic dilatancy	Overall dilatancy
S_1	Plastic dilatancy	Ultimate limit of dilatancy
c_1	Plastic dilatancy	Threshold limit of dilatancy

The volumetric strain increment due to the dilatancy in Eq.(5) is given as the function of plastic shear work. At each stage of deformation process under transient and cyclic loads, increment in plastic shear work is computed. The volumetric strain increment is given from the state parameter, which is based on cumulated plastic shear work. Ten parameters are needed for the present model: two of which characterize elastic properties of soil, another two specify plastic shear behavior, and the rest characterize dilatancy, as shown in **Table 1**.

(2) Finite element modeling

The finite element mesh shown in **Figure 6** was used for the analysis under plane strain conditions. A total of 586 nodal points and 840 elements including pore water elements were used. Five types of elements were used in the analysis: linear elements for the caisson, nonlinear elements for sand and clay, beam elements for the steel cellular structure, liquid elements for water, and joint elements for the boundaries between soil and structure. Liquid elements was used as the sea water (incompressible fluid) and was formulated as an added mass matrix based on the equilibrium and continuity of fluid at the solid-fluid interface[7]. Input parameter for liquid element was given as the density of water (1.0). Joint element was used at the interface between concrete caisson and soils or steel cellular and soils to make it possible to express the slippage at the interface. Input parameter

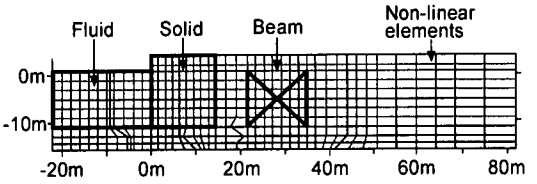

Fig.6 The mesh for finite element analysis.

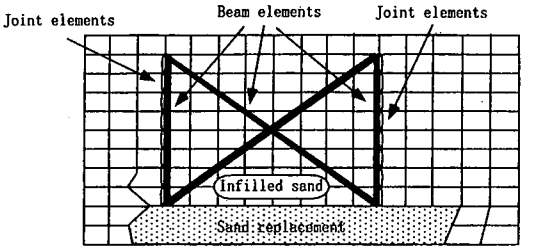

Fig.7 Schematic figure for the modeling of cellular structure.

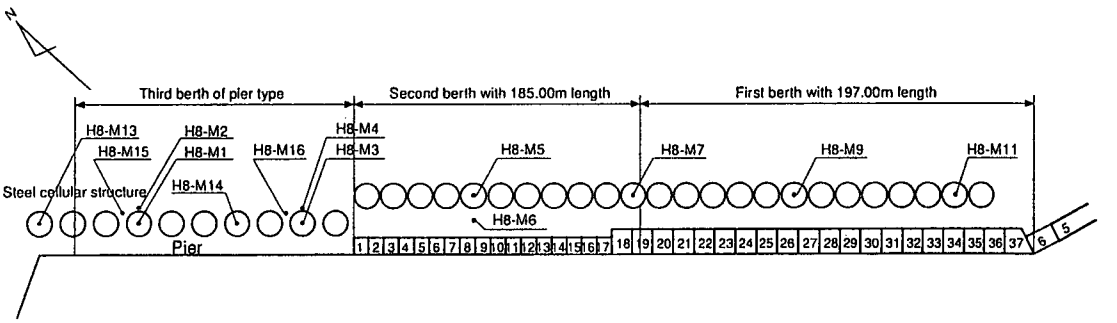

Fig.8 Location of the geotechnical investigations at the Maya Wharf.

for joint elements is friction angle and was given as 15° and 31° for vertical and horizontal direction based on the friction angle used in design standard. The computer program code named FLIP (Finite element analysis of Liquefaction Program) was used in this analyses[5].

Modeling of the steel cellular structure is one of the most difficult points to be discussed. In this paper, we assume the cellular structure possesses enough strength and rigidity to perform as a rigid block. The cellular structure consists of two vertical rigid beam elements pinching soil elements in between and two diagonal rigid beam for additional strength as shown in **Figure 7**. Continuity of soil elements inside the cellular structure and beneath the cellular structure was kept in this modeling. Joint elements at the front and back outside surface of the cellular structure can express slip or separation between the cellular structure and soil. The validity of modeling is examined in the comparison with analyzed cases with and without the cellular structure in the later chapter.

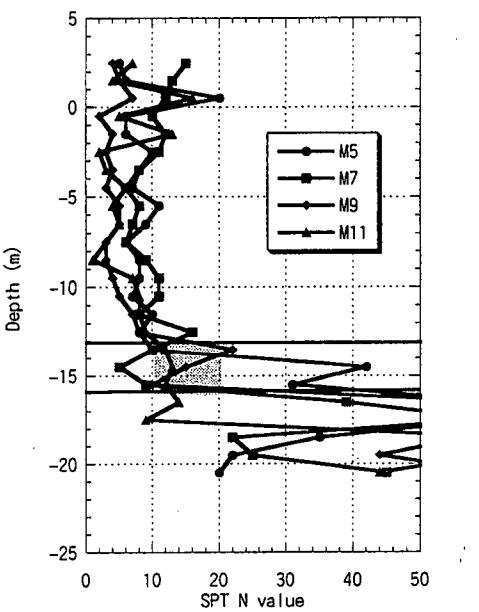

Fig.9 SPT N values investigated at the Maya Wharf No.1 and No.2 berth. (caisson type berths)

(3) Model Parameters

The model parameters were estimated by referring to the Geotechnical investigation results. **Figures 8** and **9** show the locations and results of the Geotechnical investigations at Maya Wharf, respectively. The parameters for backfilled sand and the sand replacement layer were estimated based on the SPT N values for the sand replacement layer at 17 m to 20 m depth. Since SPT N values in the sand replacement layer were scattered within wide range (5 to 40), both obtained the upper and lower extre-

Table 2 Parameters used for the analyses.

Layer No.	γ (kN/m^3)	G_a (kPa)	K_{ma} (kPa)	σ_{ma} (kPa)	ϕ_f (deg.)	ϕ_p (deg.)	Parameters for dilatancy				
							S_1	w_1	p_1	p_2	c_1
Filled sand	19.60	67620	176000	98.0	39.4	28	0.005	6.5	0.5	1.0	2.10
Sand replacement	19.60	67620	176000	98.0	39.4	28	0.005	6.5	0.5	1.0	2.10
Filled rock	19.60	180000	469000	98.0	40.0						
Mound rock	19.60	180000	469000	98.0	40.0						
Clay layer	16.66	74970	195500	143.0	30.0						

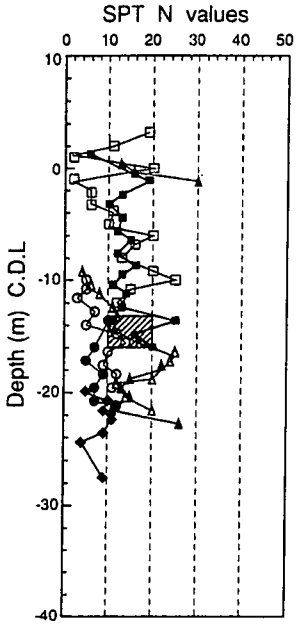

Fig.10 SPT N values in Port Island.

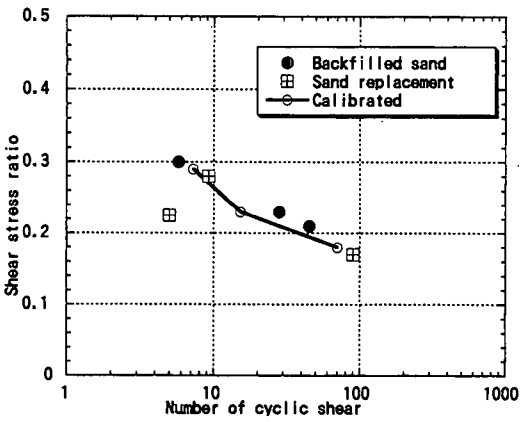

Fig.11 Computed liquefaction resistance for sand replacement layer at Maya Wharf.

me values were eliminated and an SPT N value between 10 to 20 was obtained. Considering the effect of overburden pressure, the equivalent SPT N value (corrected for 65kPa overburden pressure) for the sand replacement layer is 5 to 10. Thus medium value of 8 was used for parameter calibration and the simplified method for parameter determination was applied[8].

Since it is preferable to determine the dilatancy parameters for sand based on in-situ geotechnical investigation results, the simplified method was not used for determination of parameters related with dilatancy. The dilatancy parameters for sand at Maya Wharf was estimated using trial and error fitting method to the large scale cyclic triaxial tests results from in-situ freezing sampling at Port Island, where was reclaimed with almost the same sand as that used at Maya Wharf. SPT N values of backfilled sand and replacement sand in Port Island are shown in **Figure 10**. For the same depth as the sand replacement at Maya Wharf (K.P.-13m to -16m), SPT N values from Port Island are scattered between 10 and 20, which indicates almost the same equivalent SPT N value as the sand replacement layer at Maya Wharf. Therefore, we assumed the liquefaction resistance for the sand replacement layer at Maya Wharf and Port Island are identical.

It should be noted here that dilatancy characteristics of clay layer is neglected in this analysis. Though pore water pressure increase can occur even in clay layer, it will not show strong strain hardening such as cyclic mobility of sand. Therefore, we consider the hyperbolic stress-strain relation is enough to explain the behavior of clay layer. The liquefaction resistance for sand replacement layer at Maya Wharf is summarized in **Figure 11**. Since there is no difference between the liquefaction resistance for backfilled sand and sand used for replacement in Port Island, we used the same liquefaction resistance parameter for both sands in the analyses of Maya Wharf. Since the characteristics of the clayey layer might be uniform in Kobe Port, the parameters calibrated for clayey layer of Rokko Island[2] was used in this analyses. The parameters for analyses are summarized in **Table 2**.

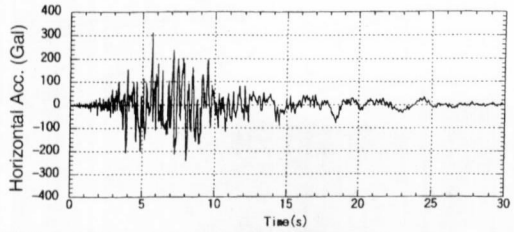

(a) Horizontal component perpendicular to the face line of quay walls.

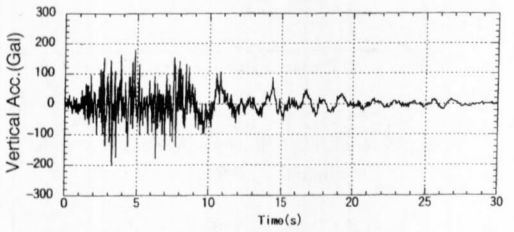

(a) Vertical component.

Fig.12 Input acceleration for the analyses recorded by Kobe City in Port Island at GL –32m.

(4) Input Accelerations

The earthquake motions was recorded by a vertical seismic array in Port Island at the ground surface and at depths of 16 m, 32 m and 83 m. The recording was successfully accomplished by Kobe City[9].

The vertical seismic array is located close to Maya Wharf, south-west direction at a distance of about 3 km. The records at the depth of 32m shown in **Figure 12** were used as the bedrock motion in the effective stress analysis. Though the depth of bedrock layer in the analysis is –16m and relatively shallow than the depth of recording station, it can be consider similar layer in this area because soil layers in this area are inclined and become deeper in south. Since the analyses were conducted in two dimensions, the earthquake perpendicular to the face line of quay wall was used for the input motion. The maximum horizontal acceleration is 311 Gal in the horizontal direction, while the maximum vertical acceleration is 200 Gal.

Before the dynamic response analysis, a static analysis was performed to simulate the initial stress distributions to take the effect of gravity into account. The same constitutive model was used as in the earthquake response analysis, but the static analysis was performed under drained conditions. With these initial conditions and the parameters mentioned earlier, an earthquake response analysis was performed on the high seismic resistance quay walls. To simplify the analysis, it was conducted under undrained conditions. The numerical time integration was made based on the Wilson-θ

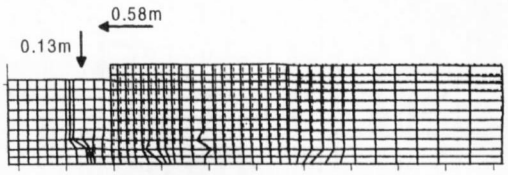

Fig.13 Computed deformation after the earthquake.

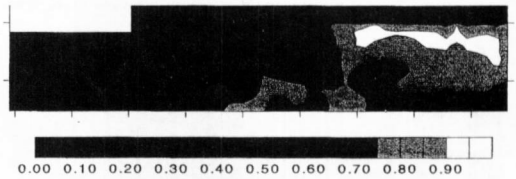

Fig.14 Computed excess pore water pressure ratio after the earthquake.

method (θ=1.4) using the time interval of 0.01 seconds. Rayleigh damping (α=0 and β=0.002) was used to ensure the stability of the numerical solution process.

4. PERFORMANCE OF HIGH SEISMIC RESISTANCE QUAY WALL

Using the aforementioned parameters, effective stress analyses were conducted. The final deformation and the excess pore water pressure ratio are shown in **Figures 13** and **14** respectively. Excess pore water pressure ratio is given based on mean confining pressure σ'_m and initial mean confining pressure σ'_{m0} as $\left(1-\sigma'_m/\sigma'_{m0}\right)$. Liquefaction behind the cellular structure was observed and the ground surface settled about 20 to 30 cm in this area. The caisson moved toward the sea and tilted slightly. Settlement of the filled rock between the caisson and the cellular structure was observed. This analysis is conducted in undrained condition and dissipation of excess pore water pressure is not considered. Therefore, computed settlement can be underestimate due to the ignorance of consolidation after liquefaction. But as for the horizontal displacement, undrained condition can be considered enough in this case since displacement of caisson mainly occurred during strong shaking duration. Furthermore, it can be considered that dissipation of pore water pressure tends to give more conservative results. The magnified deformation pattern (magnification x4) shown in **Figure 15** agrees with the observed settlements shown in **Photo 2**. Since no soil improvement was done at the seaside clayey

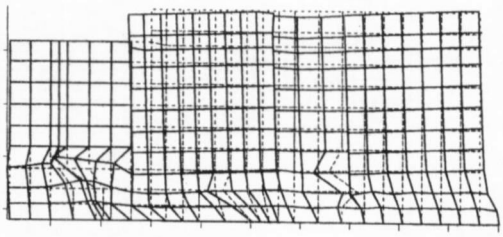

Fig.15 Deformation pattern around caisson in 4 times magnified scale.

Photo 2 Deformation and settlement between caisson and cellular structures.

layer, large shear strain of the soil elements was observed in this clayey layers and large deformation of this clayey layer occurred. Therefore, deformation can be reduced if soil improvement is conducted at the seaside clayey layer where large shear strains were observed.

Horizontal displacement at the top of the caisson was about 0.6 m toward the sea, which is fairly smaller than the observed deformation of 1.2 m. The major factor which may have reduced the deformation could be the absence of the effect of shaking parallel to the face line of the quay wall. Since the analysis was conducted in two dimensions, earthquake motion parallel to the face line of quay wall, which is the predominant direction of earthquake shaking, can not be considered. But liquefaction resistance of soils might be affected by this parallel shaking. Therefore, in this analysis, liquefaction resistance might be overestimated since we consider only one-directional shaking in the horizontal plane which is least likely cause liquefaction. In order to consider the effect of earthquake motion parallel to the face line, liquefaction resistance under multiple directional shear should be considered.

Some research exists on liquefaction resistance

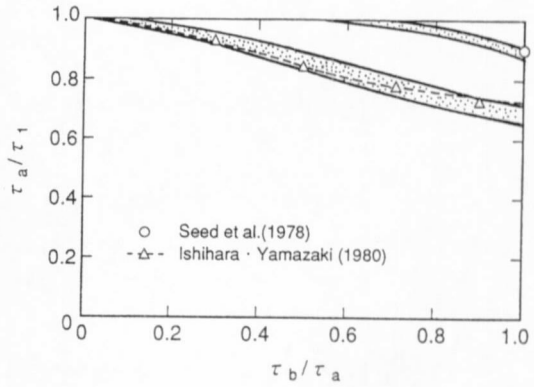

Fig.16 Reduction of liquefaction resistance under multiple shear (after Yoshimi, 1991)

under multiple directional shear and the results are summarized in **Figure 16**[10]. In **Figure 16**, the horizontal axis shows the ratio of shear stress in two directions, τ_b/τ_a, and the vertical axis indicates the ratio of shear stress in two directional shear, τ_a, and one-directional shear. Here, τ_a is the greater one in two directional shear. τ_1 is the one-directional shear component which would cause liquefaction equivalent to that caused by the combination of two-directional shear τ_a and τ_b. The triangle marker in **Figure 16** shows the test results for saturated sand and circle shows the estimated value from the test results of dry sand. The dark hatched area in **Figure 16** shows the area of calculated values using test results. Though the results are scattered, the research indicates that liquefaction resistance under two-directional shaking is 10 to 30% lower than that under one-directional shaking.

The analysis of Maya Wharf is more complicated than the situation represented by the analytical modeling. The motion parallel to the face line of the quay walls is greater than the perpendicular motion, which is used in the analysis. Therefore liquefaction resistance might be significantly lower than predicted, possibly more than 30% lower than predicted by the one-directional shaking analysis. A series of parametric analyses with liquefaction resistance reduced by 10 to 40% were conducted. Reduced liquefaction resistance is shown in **Figure 17**. To consider the effects of the existence of the old steel cellular structure, a series of analyses without steel cellular elements (beam and joint elements) were also performed. Computed horizontal displacement under various levels of liquefaction resistance is shown in **Figure 18**. The calculated displacement agrees with the observed dis-

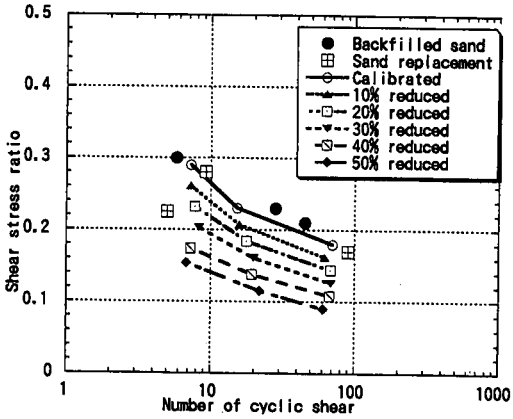

Fig.17 Reduced liquefaction resistance for parametric study.

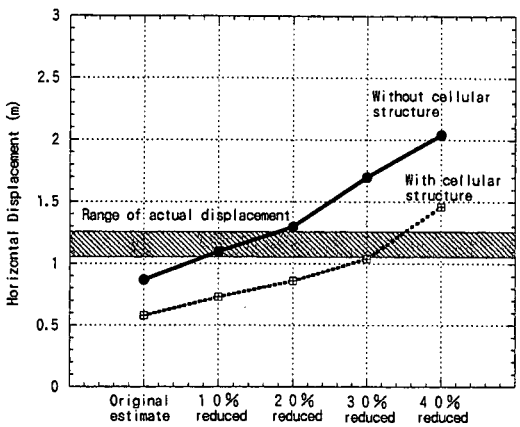

Fig.18 Computed horizontal displacement under various liquefaction resistance, with and without cellular structure.

placement (indicated a dark hatch) when the analysis is performed using a 30 to 40% reduction in liquefaction resistance in case with steel cellular structure. The dotted line shows the displacement without the cellular structure and indicates that the displacement without the cellular structure is about two times the displacement with the cellular structure. The displacement with the cellular structure is probably underestimated since the cellular structure is assumed to be rigid block. Therefore, the actual performance of the quay wall is probably somewhere in between the performance predicted with and without the cellular structure.

5. HIGH SEISMIC RESISTANT DESIGN OF QUAY WALLS

(1) The effect of high seismic resistant design

To consider the effect of high seismic resistant design, computed displacement of the high seismic

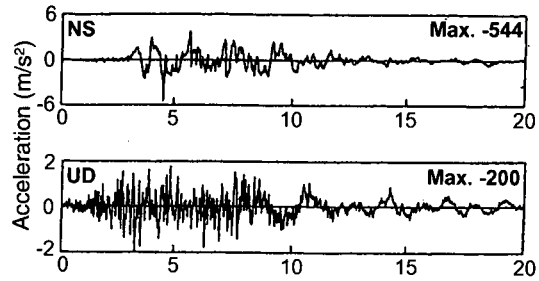

Fig.19 Input acceleration for the analyses recorded by Kobe City in Port Island at GL -32m.

resistance quay walls without the cellular structure and computed displacement of usual type quay walls are compared. The -14m type quay walls at the south end of Rokko Island designed with a seismic coefficient of 0.15 were analyzed as usual type quay walls. The details of the analyses on these quay walls were reported by Iai et al[2].

To consider the most severe condition, the recorded motion at Port Island in the N-S direction, maximum 544 Gal, which is close to the horizontal predominant direction of motion, was used as input ground acceleration for the analyses. The input motion is shown in **Figure 19**. A parametric study of input acceleration levels of 100, 200, 300, 400 and 544 Gal was conducted. For liquefaction resistance, two series of analyses using non-liquefiable soil and liquefaction resistance estimated by the in-situ freezing sampling were conducted. Non-liquefiable soil means soil material without considering dilatancy characteristics. It gives hyperbolic stress-strain relationship as we used for clay layers. Here, the results of in-situ freezing sampling in Port Island were used for the high seismic resistant designed case as mentioned earlier and the results of in-situ freezing sampling in Rokko Island were used for the usual quay wall case. As mentioned earlier, there is no soil improvement at the seaside clayey layer under the caisson in the high seismic resistant designed case and large deformation can be induced. Therefore, in the case with the high seismic resistance quay wall with non-liquefiable soil, we assume the soil improvement in the seaside clayey layer under the caisson was done and the same material parameters for the sand replacement layer were used. The area near the seaside basement that is assumed to be improved is shown in **Figure 20**.

The results of numerical parametric study are shown in **Figure 21**. Deformation of the high seis-

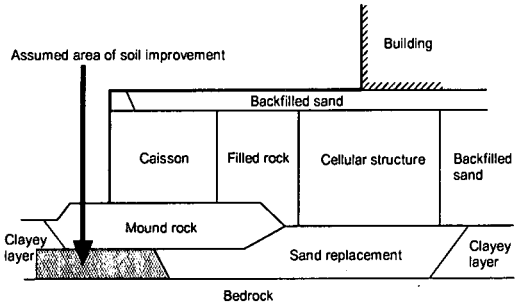

Fig.20 Assumed area of soil improvement at the seaside bottom of caisson.

mic resistance quay walls with no liquefaction does not increase until the maximum input acceleration exceeds 200 Gal. On the other hand, the deformation of the usual caisson type quay walls with no liquefaction increases linearly just after the maximum acceleration exceeds 200 Gal.

Discussed maximum acceleration is defined in the basement rock and there is no apparent relation with static seismic coefficient used in design. But Noda, Uwabe and Chiba presented an empirical relation between observed maximum acceleration on ground and equivalent seismic coefficient. Noda and Uwabe's empirical formulation is summarized as follows[11].

$$K_e = \frac{\alpha}{g} \qquad (\alpha < 200Gal) \qquad (10)$$

$$K_e = \frac{1}{3}\left(\frac{\alpha}{g}\right)^{\frac{1}{3}} \qquad (\alpha \geq 200Gal) \qquad (11)$$

where

K_e : Equivalent seismic coefficient acting on quay walls

α : Maximum acceleration at the ground surface in SMAC equivalent type acceleration

g : Gravity acceleration

SMAC equivalent type acceleration is equivalent to the acceleration recorded by the SMAC accelerograph and it can be computed by the SMAC equivalent filter.

Therefore, the equivalent seismic coefficient can be estimated using the computed maximum acceleration at the ground surface. We used both the equivalent linear method and the effective stress analysis method to compute the maximum acceleration at the ground surface. The estimated equivalent seismic coefficients are summarized in **Figure 21** as a reference of maximum input acceleration level at the base rock. The 100 Gal acceleration level in the base rock is amplified to 110 to

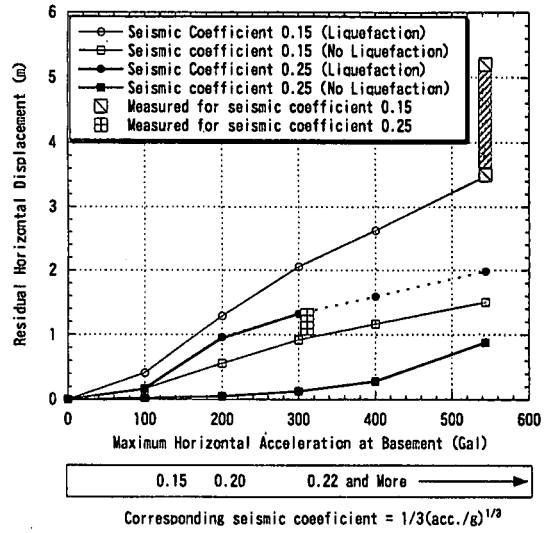

Fig.21 Horizontal displacement under various input acceleration levels.

130 Gal in SMAC equivalent acceleration at the ground surface and equivalent to seismic coefficient 0.11 to 0.13. It follows that the usual type quay walls designed with seismic coefficient 0.15 remain at a small deformation level for this level of acceleration. When the input acceleration level at the bedrock exceeds 200 Gal, no major amplification of acceleration at the ground surface is observed due to the effect of non-linearity of soils. Furthermore, when input acceleration at the bedrock exceeds 300 Gal, maximum acceleration at the ground surface remains constant at about 300 Gal in SMAC equivalent acceleration. It means the equivalent seismic coefficient never exceeds 0.22 or 0.23 in this case, and it is difficult to discuss the equivalent seismic coefficient when the input acceleration level at the basement rock exceeds 300 Gal.

The minimum acceleration level that causes damage for a given seismic coefficient can be estimated from **Figure 21**. For example, in non-liquefaction case, the minimum acceleration level to cause the damage of 1.0m deformation level for the usual type quay walls designed with seismic coefficient 0.15 is about 300 Gal and for high seismic resistant type designed with a seismic coefficient of 0.25 is about 550 Gal. In **Figure 21**, observed displacements of the quay walls at Rokko Island and Maya Wharf are shown, and the displacement agree with the computed deformation considering liquefaction. As mentioned earlier, we consider the orientation of the face line of high seismic resistance quay walls, and 30% reduced liquefaction resistance was used

for the high seismic resistant case. Therefore, it is impossible to use input motion of 400 Gal or more, since we assume 700 Gal or more acceleration for the parallel direction of face line in this case. This is the reason the deformation with the input motion over 300 Gal are shown with dotted line in **Figure 21**.

When liquefaction countermeasures were completely done, displacement of quay walls was fairly reduced. Especially for the high seismic resistant case, the displacement is only about 30 cm for 400 Gal input and only about 90 cm for 544 Gal input. These results indicate that the effectiveness of the high seismic resistant design is increased when liquefaction countermeasures are completely conducted.

(2) Level of improved liquefaction resistance

To consider the effect of liquefaction countermeasures, we used the idealized non-liquefiable sand for the aforementioned analyses. Since not only liquefaction resistance but also soil properties such as shear modulus might change when liquefaction countermeasures are conducted, it is necessary to consider the effect of liquefaction countermeasures themselves and the desirable level of soil improvement.

SPT N values are often used for the evaluation of soil properties including liquefaction resistance since other methods are more expensive or lack reliability. In this case, an equivalent SPT N value corrected for 65 kPa overburden pressure is used for port structures design. Since a simplified method for parameter calibration in FLIP program using equivalent SPT N value is presented[8], we conducted the parametric study considering the level of liquefaction countermeasures using equivalent SPT N values. The results under equivalent SPT N values of 5, 10, 15, 20 and 25 are summarized in **Figure 22**. The high seismic resistance designed quay walls at Maya Wharf and recorded NS directional motion at Port Island with maximum acceleration of 544 Gal were used for this parametric study. If the equivalent SPT N value exceeds 20, residual horizontal displacement remains under 1.0 m which shows good seismic performance. It can be concluded that quay walls designed with a seismic coefficient of 0.25 and liquefaction countermeasures at the level of equivalent SPT N value of 20 can survive under the great earthquake motion of peak bedrock acceleration of 544 Gal.

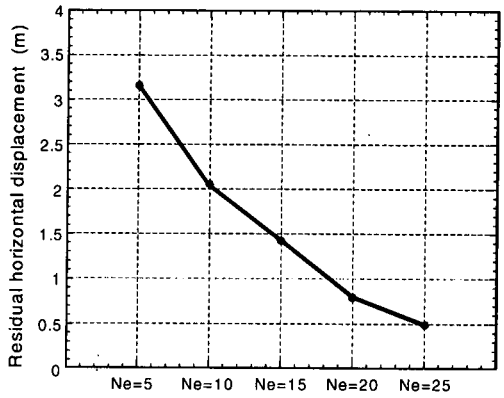

Fig.22 Horizontal displacement related to the equivalent SPT N values.

6. CONCLUSION

Two-dimensional effective stress analyses for high seismic resistance quay walls at Maya Wharf were conducted. The performance of the quay walls is summarized as follows.

(1) Computed deformation is smaller than observed deformation. This might be due to the effect of multidirectional shaking on liquefaction resistance, which is neglected in the two-dimensional effective stress analyses. Reducing the liquefaction resistance by 30% results in a predicted deformation that agrees with the observed deformation.

(2) The existence of the steel cellular structure behind caisson walls reduced the deformation. Without the cellular structure, the observed deformation might be amplified about two times.

(3) The observed deformation of the high seismic resistance quay walls at Maya Wharf are mainly caused by liquefaction in the sand replacement layer and filled sand behind the quay walls. Therefore, adequate liquefaction countermeasures can limit the deformation. It can be considered reasonable that current Japanese design standard for port and harbour structures requiring adequate liquefaction countermeasures in case of the possibility of liquefaction.

(4) The minimum input acceleration required level for deformation to occur increases when the quay walls are designed with large seismic coefficients. This trend is clear when liquefaction countermeasures are conducted. The quay wall with large seismic coefficient and adequate liquefaction countermeasures have fairly good seismic performance. For example, even with a large input motion with maximum acceleration of 544 Gal, horizontal displacement at the top of the quay walls can remain

under 1.0 m if liquefaction countermeasures are completely done.

REFERENCES

1) Inagaki, H., Iai, S., Sugano, T., Yamazaki, H., and Inatomi, T.: Performance of caisson type quay walls at Kobe port, *Special Issue of Soils and Foundations*. pp.119-136, 1996.
2) Iai, S., Ichii, K., Liu, H. and Morita, T.: Effective stress analyses of port structures, *Special Issue of Soils and Foundations*, Japanese Geotechnical Society, pp.97-114, 1998.
3) Sugano, T., Morita, T., Mito, M., Sasaki, T. And Inagaki, H.: Case studies of caisson type quay wall damage by 1995 Hyogoken-nambu earthquake, *Proceedings of eleventh world conference on earthquake engineering*, Acapulco, Mexico. (CD-ROM), 1996.
4) Sato, Y., Ichii, K., Sato, Y., Hoshino, Y., Miyata, M., Morita, T. and Iai, S.: Strong-motion earthquake records on the 1995 Hyogo-ken nambu earthquake in port areas, *Technical note of the Port and Harbour Research Institute*, No. 907, 1998.
5) Iai, S., Matsunaga, Y and Kameoka, T.: Strain space plasticity model for cyclic mobility, *Soils and Foundations*, Vol. 32, No. 2, pp.1-15, 1992a.
6) Iai, S., Matsunaga, Y. and Kameoka, T.: Analysis of cyclic behavior of anisotropically consolidated sand, *Soils and Foundations*, Vol. 32, No. 2, pp.16-20, 1992b.
7) Zienkiewicz, O.C.: The Finite Element Method, 4th edition, McGraw-Hill Book Co, vol. II, pp.407-419, 1977.
8) Morita, T., Iai, S., Liu, H., Ichii, K. And Sato, Y.: Simplified method to determine parameter of FLIP, *Technical note of the Port and Harbour Research Institute*, No. 869 (in Japanese), 1997.
9) Sugito, M., Sekiguchi, K., Yashima, A., Oka, F., Taguchi.Y and Kato, Y.: Correction of orientation error of borehole strong motion array records obtained during the South Hyogo Earthquake of Jan.17, 1995, *Journal of Structural Mechanics and Earthquake Engineering*, No. 531, I-34, JSCE, pp.51-63, 1996.
10) Yoshimi, Y.: Liquefaction of Sandy Deposit, *Gihoudo Press*, 2nd edition, pp.86 (in Japanese), 1991.
11) Noda, S., Uwabe, T. and Chiba, T.: Relation between seismic coefficient and ground acceleration for gravity quay wall, *Report of the Port and Harbour Research Institute*, Vol. 14, No. 4, pp.67-111 (in Japanese), 1975.

(Received August 30, 1999)

耐震強化岸壁の耐震性能

一井康二・井合　進・森田年一

震災時に備える防災拠点の施設として耐震強化岸壁が日本各地に建設されている．こういった耐震強化岸壁の有効性については兵庫県南部地震時に摩耶埠頭岸壁が無被災であった事例が知られているが，一般の耐震強化岸壁の耐震性能がどの程度のレベルにあるかは必ずしも明らかにされていない．そこで，有効応力解析により兵庫県南部地震時の摩耶埠頭岸壁の無被災メカニズムを明らかにし，一般の耐震強化岸壁の耐震性能を検証した．有効応力解析の結果，摩耶埠頭岸壁の変位量におよぼした岸壁法線の方向性・ケーソン背後に埋め殺しされたセルの存在の影響が明らかになった．また，液状化対策の実施によりシビアな荷重条件下でも耐震強化岸壁の変位量は1m以下に抑制できるとの見通しが得られた．